DOI: 10.1002/chem.200600307

Visual Artificial Tongue for Quantitative Metal-Cation Analysis by an Off-the-Shelf Dye Array

Jae Wook Lee,[a] Jun-Seok Lee,[a] Mira Kang,[a] Andrew I. Su,[b] and Young-Tae Chang*[a]

Abstract: A chemical-probe array composed of 47 off-the-shelf dyes was prepared in solution format (New York Tongue 1: NYT-1) and was tested in the identification and quantitation of 47 cation analytes, including 44 metal ions, in addition to H^+, NH_4^+, and tetrabutylammonium (TBA). The cation solutions were tested in a series of concentrations and the fold-change in effective absorbance was analyzed by principal-component analysis (PCA), hierarchical-cluster analysis (HCA), and nearest-neighbor decision to determine both identity and quantity of the analytes. Apart from alkali-metal ions (Na^+, K^+, Li^+, Cs^+, and Rb^+), which behave very similarly to each other due mainly to their low response, most of the cations were clearly distinguishable at 10 mM concentration. The practical detection limit of each analyte was also determined by a sequential dilution and the nearest-neighbor decision method. In the finalized working analyte concentration range (approximately 10 mM down to 0.33 μM), by considering alkali metals as one analyte group, most of the analytes were correctly identified (99.4%). Furthermore, the success rate at which the concentration of each analyte was correctly determined was also high (96.8%).

Keywords: alkali metals · cations · dyes/pigments · hierarchical-cluster analysis · principal-component analysis

Introduction

Organic dyes that change color in response to analyte(s) have been used as optical/visual sensors for more than one hundred years.[1] This colorimetric test is attractive because the color change can be detected with the naked eye, thus, no instrumentation is required, and some degree of quantitative analysis is often possible. Photometric measurements of color intensity at defined wavelength(s) enable the systematic quantitative analysis of the analytes by comparison with calibration curves. These conventional approaches to chemical sensors exploit usually a one-analyte-versus-one-sensor methodology, hopefully without interference by other elements in the sample. Thus, in most cases, the main issue is the selectivity of the sensor toward only the target analyte, which is highly challenging.

Our taste and smell sensory organs (tongue and nose) possess between dozens and hundreds of receptors[2] and can differentiate and identify tens of thousands of different tastes and smells by analyzing the unique patterns of response generated by each receptor. Notably, in this pattern analysis, each individual receptor does not need to be specific or selective to a given analyte for identification to be successful. Inspired by this combinatorial sensing approach of Mother Nature, many artificial sensory systems using multiple probes or sensor arrays based on electronic or optical measurements have been developed.[3,4] Although most studies required a careful rational design and synthesis of receptor/probe molecules, commercially available off-the-shelf dyes were also used successfully in the discrimination of multiple analytes. For example, Sessler et al. reported a colorimetric anion probe composed of commercial dye solutions combined with qualitative naked-eye detection.[5] Suslick et al. used organic indicator dyes spotted on a hydrophobic surface for various analytes,[6,7] and the color change was monitored in terms of RGB (red, green, blue) color values for systematic quantitative analysis. In contrast to the solid-surface-assisted dye arrays, more-conventional solution-phase analysis has its own unique advantages, especially if the analyte is in liquid form, that is, in tongue format.

[a] J. W. Lee, J.-S. Lee, Dr. M. Kang, Prof. Y.-T. Chang
Department of Chemistry, New York University
New York, NY 10003 (USA)
Fax: (+1) 212-995-4203
E-mail: yt.chang@nyu.edu

[b] Dr. A. I. Su
Genomics Institute of the Novartis Research Foundation
10675 John Jay Hopkins Drive, San Diego, CA 92121 (USA)

Supporting information for this article is available on the WWW under http://www.chemeurj.org/ or from the author.

These include the non-requirement of probe immobilization, homogeneous interaction of analyte with probes, fast kinetics of analyte delivery to probes, and the availability of quantitative spectrophotometric measurement by using standard 96- or 384-well (or even higher density) microtiter-plate readers. Although these advantages are known, the systematic acquisition and processing of large amounts of data for a solution-dye-probe array, especially against large numbers of analytes, has not yet been fully exploited. For example, Wolfbeis et al. used eight fluorescence indicators to analyze five metal cations,[8] and Mueller-Ackermann et al. used seven fluorescence chelators for the determination of mixtures with four heavy-metal cations.[9] Niessner et al. used four fluorescence dyes to analyze quantitatively seven metal cations,[10] and Suzuki et al. used three metallochromic dyes on three metal cations for qualitative and quantitative analysis by neural network inversion.[11] Herein, we report the construction of a universal probe array by using off-the-shelf commercial dyes and we demonstrate its systematic application to the extensive analysis of metal cations covering most of the commercially available metal cations.

Results and Discussion

To select desirable probe-array components, 140 commercial dyes, including triphenyl, azo, naphthyl, acridine, and hydroquinones, some of which are known indicators for various organic and inorganic analytes, were collected and tested for their sensing performance against a broad range of metal cations. For reproducible spectrophotometric data acquisition, the test solution must be homogeneous over the measurement period and the color change should be fast and sustained. By using these criteria, the 47 most-sensitive and stable dyes were selected (the details of the selection procedure are given in the Experimental Section, see also Figure S1). Following the convention of naming a dye with a color and the area of its production, we dubbed our dye array "New York Tongue 1 (NYT-1)."

Metal cations are accompanied by counteranions, and it is possible that the probe response is due not only to cations, but also to anions. We tested a series of sodium and tetrabutylammonium (TBA) salt solutions with various anions, such as halide, acetate, nitrate, perchlorate, sulfate, and phosphate in NYT-1. Interestingly, halides (except fluoride) and nitrate showed minimal responses to NYT-1 in both Na^+ and TBA salts, whereas other anions showed high responses. Considering the solubility and stability of the salts in water, we selected nitrate as the anion counterpart and collected 44 commercially available metal nitrates in addition to nitric acid (H^+), ammonium nitrate (NH_4^+), and TBA-nitrate for comparison (Figure S2). For the demonstration of distinguishing cation identity, we used 42 cations that were fully soluble at 10 mM concentration. The absorbance spectra were measured in 384-well-plate format, and the fold-change of absorbance for each dye at its λ_{max} was calculated for quantitative analysis (see details in Experimental Section). The log value of fold-change, "log*F*" was used for principal-component analysis (PCA) and hierarchical-cluster analysis (HCA).

PCA is a mathematical transformation that reduces the dimensionality of the data sets by transforming to a new set of variables.[12] The PCA results of all 42 cations along with their pH profiles is presented by the first two principal components in Figure 1A. Four independent data sets of individual cations were plotted close to or overlapping with each other, which demonstrated the low error range and the high reproducibility of the experiment.

First of all, it was apparent that alkali-metal ions (Na^+, K^+, Li^+, Cs^+, and Rb^+) were clustered very closely to each other and were practically indistinguishable (zoomed picture in Figure 1B). It seems this is due mainly to the intrinsic low response of alkali-metal ions to the probe dyes and, thus, all the spots in PCA are positioned close to the control spot (water). NH_4^+ (Amm) also showed a low response, however, it was clearly distinguishable from the alkali metals in PCA.

Another interesting group of analytes in the PCA plot were the lanthanide metal ions (La^{3+}, Ce^{3+}, Sm^{3+}, Eu^{3+}, Gd^{3+}, Tb^{3+}, Dy^{3+}, Ho^{3+}, Er^{3+}, Lu^{3+}), which may reflect their similar chemical properties, at least in terms of their interaction with the probe dyes (Figure 1C).

Notably, the pH-profile spots are separated completely from the cation spots and are fully distinguishable from any of the metal cations (Figure 1A). Although it was apparent that the pH effect was reflected in our PCA data (most of the known metal indicators respond to pH), this full separation of each analyte demonstrates clearly that the interaction of cations with NYT-1 also generates unique pH-independent patterns. One alternative possibility may be the use of buffer solution to suppress the pH effect. However, we decided to use simple water, for the following reasons. Firstly, the pH difference itself provides important information for each analyte and we actively accommodate the properties into the analysis as a parameter. Secondly, the range of buffers is too large and depends on their composition (cations and anions) and pH, which can potentially interfere with the measurements. Thirdly, different buffers permit different solubilities for each metal nitrate, which limits the universality of the analyte type and concentration. Lastly, if real-world sample application is concerned, a minimum change in the analyte sample is desirable without additional sample preparation, that is, buffering.

In parallel with PCA, the log*F* data were also analyzed by HCA, another popular clustering analysis method that is widely used for microarray data analysis.[13] Results of agglomerative hierarchical-clustering, along with heat-map analysis results in four replicating data sets are summarized in Figure 2. The lengths of the horizontal lines represent their relative differences in terms of Euclidian distance. Most of the metal cations are clearly separated, except the alkali-metal ions, which are all overlapped and are not distinguishable. NH_4^+ groups were embedded in the middle of

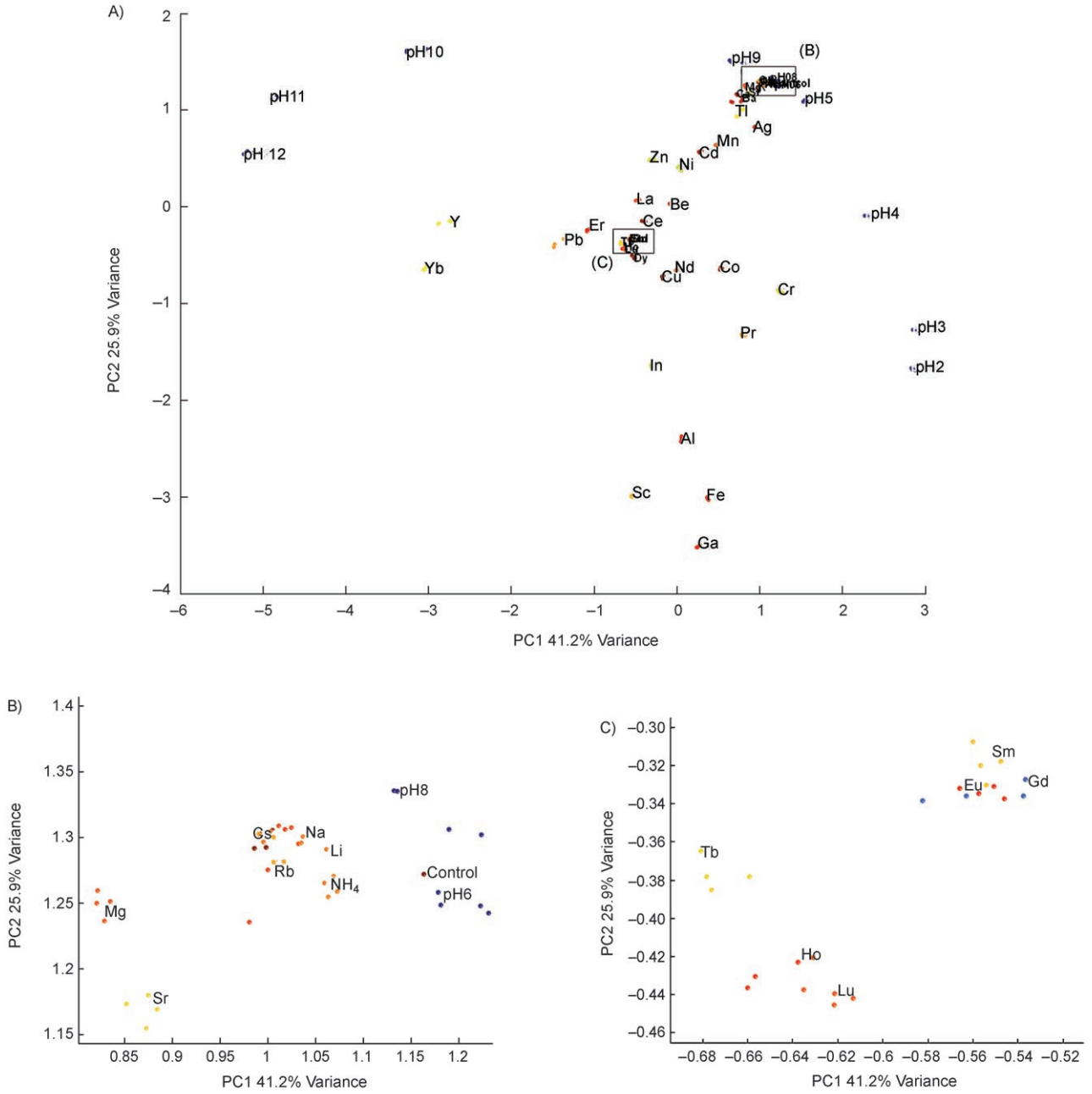

Figure 1. Principal-component analysis. A) PCA results with 42 analytes at 10 mM (data of four repeated experiments). First principal component has 41.2% variance, second principal component has 25.9% variance. First two components cover 67.1% variance. B) Enlargement from (A) for alkali metals that are grouped in narrow region. (C) Enlargement from (A) for lanthanide metals.

alkali-metal clusters, but a separate cluster for NH_4^+ was still identified. Considering both the PCA and HCA results, the five alkali-metal ions were bundled together as one analyte group, marked as "alkali." With the exception of the alkali-metal ions, only Gd^{3+} was partially co-clustered with Eu^{3+}.

Although both PCA and HCA are useful visualization tools, they cannot present the full comparison in the two-dimensional figures shown. For a simple quantitative analysis, we decided to use the "nearest-neighbor decision" method[14] by using Euclidian distances between data sets. For each data set (test set), the Euclidian distances were calculated from 167 other data sets (42 cations × four experiments−the one test set itself). If two data sets are identical (in case the fold-change is the same for every dye), the Euclidian distance is zero. The data set with the lowest Euclidian distance was selected as the best candidate for the test set, and these two identities were compared to make a "true" or "false" judgment. Permitting five alkali metals as one group (labeled as "alkali"), from the 168 test sets, only

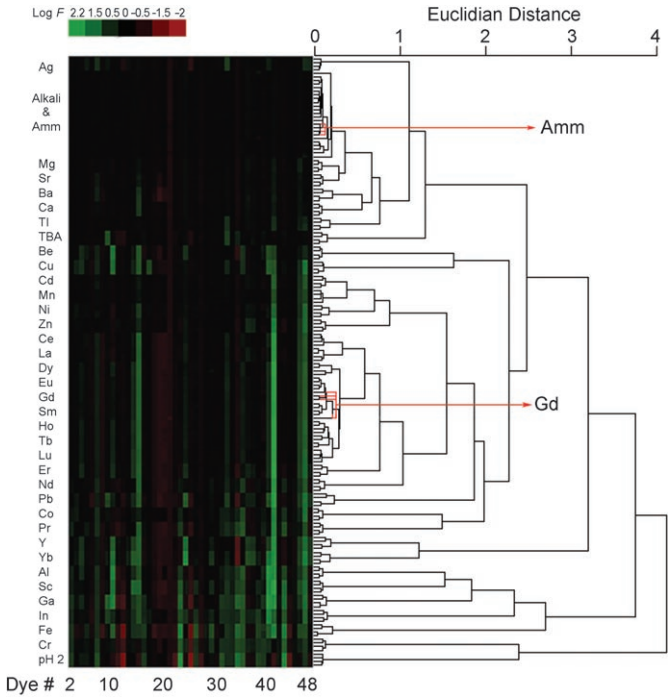

Figure 2. Heat map (left) and agglomerative hierarchical-clustering analysis (right) of cations at 10 mM. Heat map shows the pattern of responses of the 47 dyes (horizontal axis) to the 42 cations, including five alkali metals (vertical axis) for quadruple experiments. Green represents positive values of log*F*, red represent negative values.

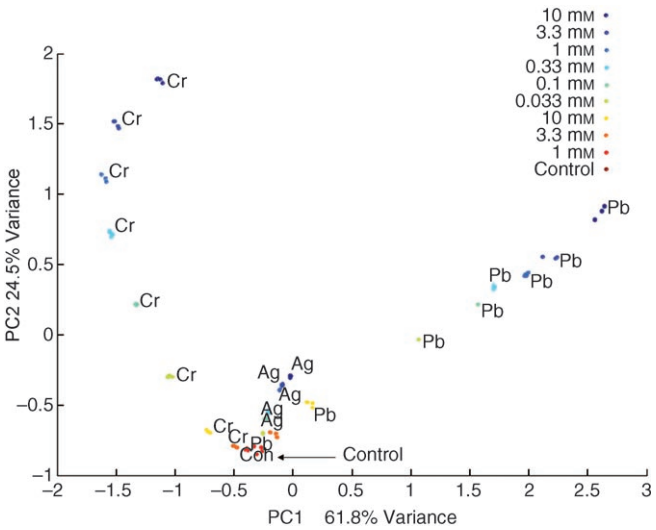

Figure 3. Concentration profile obtained by PCA with three cation analytes. The red-brown point is the control point, which represents, theoretically, no response to any dye.

one "false" was found in one set of Gd (misidentified as Eu), and three other Gd sets made "true".

Encouraged by the high accuracy of the identification of 42 cations at 10 mM concentration, our next challenge was the quantitation of the analytes. The above 42 cations were tested at a series of concentrations obtained by sequential dilutions of approximately three-fold, that is, 10, 3.3, 1.0, 0.33, 0.1, 0.033, etc. mM, until the dye response was approaching zero. In addition, five more cations (Bi^{3+}, Hg^{+}, Hg^{2+}, Pd^{2+}, Tl^{3+}) that were not included previously due to their lower solubility were now added to the test; the highest concentration for Hg^{2+} was 3.3 mM, and for the other four cations it was 0.33 mM. Most of the dyes were tested down to 1 μM or even lower for several sensitive cations.

Initially, we tried to analyze all of the data by PCA and HCA for each individual ion at different concentrations. Clear concentration-dependent patterns were observed for all of the analytes, and three examples (Ag^{+}, Cr^{3+}, Pb^{2+}) plotted by PCA are shown in Figure 3. As the concentration decreases, the PCA spot approaches the control (water). Although plotting all the data in one graph makes a visual analysis difficult, the PCA plot for each analyte will serve as a multidimensional standard curve for concentration determination.

To simplify the quantitative analysis, we applied the "nearest-neighbor decision" to both the identification and quantitation. At low concentrations, many of the data sets generated "false" scores, due mainly to the low response to the dyes. To determine the practical range of the analyte detection, we trimmed off the "wrong" scored data sets starting from the lowest concentration by applying the following criteria; each analyte at a given concentration was tested four times, and if three or four data sets give "true" scores, then the whole group was scored as "true", if not, "false". This tolerance accommodated an experimental error, such as a pipetting error, that occurred in only one individual well. This procedure was repeated until all the "wrong" low-concentration data sets were removed. The final practical detection ranges (10 down to 0.33 μM) of each analyte are summarized in Figure S5.

From a total of 1320 surviving data sets (330 data groups with four repeats), 1286 (97.4%) gave the correct identity of the analytes, and 1260 (95.5%) gave correct answers for both identity and concentration. Most of the 26 cases with correct identity, but wrong concentration, were found at the low-concentration range, and the degree of error lay within one concentration step higher or lower. By considering 330 groups and by using the same criteria of three or four "true" out of four, 308 (99.4%) gave the correct identity, and 300 (96.8%) gave correct answers for both identification and concentration.

Conclusion and Perspectives

By carefully testing a total of 140 off-the-shelf dyes in terms of response time, precipitation, and color change upon analyte treatment, 47 dyes were selected for artificial tongue (NYT-1), and these were tested for 47 cation analytes, including 44 metal ions. Following optimization of the analysis method, we determined the practical concentration range of detection for each individual cation with a high success rate of identification and quantitation. By using this standard

data set, any concentration (within this range) of nitrate cation can, in principle, be analyzed for both identity and concentration. If comparison of one data point (zero dimension) is insufficient for certainty, the data set from a sequential dilution of the unknown sample will allow comparison of the concentration-dependent curve (one dimension) for more-accurate analysis.

Although the first demonstration of NYT-1 was conducted for cation analytes, this artificial tongue and its analysis method can, in principle, be extended easily to any other organic/inorganic analytes, and also to multicomponent mixture samples. Although we have selected "nitrate" as an anion partner for our current cation study due to its exceptionally low response to NYT-1, the real-world samples may contain various kinds of anions that may affect significantly the response of our tongue, thereby making their analysis more complicated. By using the established procedure reported here, we will study systematically the anion effects as the next step in the general application of our tongue. Based on the selectivity of the probes toward different classes of analytes, either numerical analysis or further selection of dye sets will hopefully provide a universal and practical tongue for the qualitative and quantitative application to real samples.

Experimental Section

Materials and general methods: The spectroscopy grade of dimethyl sulfoxide (DMSO, 99.9% purity) was purchased from Acros. Deionized water was prepared by using the Picosystem (filtering system) from Hydro service and the supplied company. Unless otherwise mentioned, all metal nitrates were purchased from Aldrich. $AgNO_3$ and $Bi(NO_3)_3$ were purchased from Acros, and $Cd(NO_3)_2$ was purchased from Spectrum Chemical. All dyes were purchased from Chem Service, Sigma, Fluka, Acros, Fisher, Janssen, Allied Chemical, and Aldrich. Polystyrene 384-well plates (clear, flat bottom) were purchased from Corning.

Instruments and computer software: All graphic data were recorded by using a CCD camera (Cannon; Power Shot G5) equipped with a Spectroline model CC-88 analysis cabinet. All UV/Vis spectra were recorded from 350–750 nm by using a plate reader (Molecular Device; Spectra Max Plus 384). All image analyses were performed by using Adobe Photoshop version 7.0. Principal-component analyses were performed by using MatLab version 6.5, and the hierarchical-cluster analyses were performed by using S-Plus version 6.2 Student Edition.

Probe-dye selection and optimization: A total of 140 commercial dyes, including triphenyl, azo, naphthyl, acridine, and hydroquinones, some of which are already known indicators for various organic and inorganic analytes, were collected and dissolved in dimethyl sulfoxide (DMSO, 10–100 mM) and then diluted in water. Because the relative amount of DMSO varied according to the solubility and absorbance intensity of each dye, to maintain the main aqueous environment, the DMSO ratio was maintained in all cases below 5% in water. Dyes that are not fully soluble in 5% DMSO solution were excluded at this stage.

Dye solutions (30 μL each) were loaded into the wells of a 384-well microtitre plate and equivalent volumes of various metal salt solutions were added to each well. Distilled water was used as control and the color changes were monitored over 1 h by using a CCD camera and absorbance plate reader. The absorbance of the dye solution was measured within the wavelength range 350–750 nm at 10 nm intervals. By considering the absorbance change in response to analytes, the dye concentrations were readjusted to ensure the absorbance did not exceed 1.3 at λ_{max} to avoid saturation.

We set up the criteria for selection of dyes as follows; the desirable probe dyes 1) should not form precipitates upon analyte treatment during the measurement time, 2) should change their color significantly either in wavelength or intensity, and 3) should reach the end point of color change within a reasonably short period.

The first test was precipitation. Although precipitation is a useful indication for qualitative analysis in specific analyte detection, it would disturb the absorption spectra and homogeneity of the test solution, and, thus, would generate poor reproducibility in quantitative measurement. From this aspect, the highest concentrations of metal-ion stock solutions were set as 20 mM (10 mM in final 1:1 mixtures with dyes) to avoid massive precipitation, which occurred in many combinations with higher ion concentrations. Even at 10 mM, some dyes underwent significant precipitation within an hour (e.g., mordant black 11, Figure S1a), so these dyes were removed.

The second test was color change of dyes upon analyte addition. Some dyes did not show a significant color or spectral change upon metal-ion addition (e.g., benzene-azo-1-naphthylamine, Figure S1b), so these dyes were removed from the probe list.

The third test was kinetics of color change. In view of the spectrophotometric measurement time of 20 min for one 384-well plate, the color change should be fast (5 min is our criteria), and the new color should be sustained over the next hour. Dyes that exhibit a slow development in color (e.g., pararosaniline, Figure S1c) were also removed from our candidate list.

From the dyes that satisfied the above three criteria, we selected a further final 47 dyes based on their diverse response to various analytes (e.g., mordant blue 29, Figure S1d). In addition to these 47 dyes, water was included in the array to check the intrinsic color of analytes, which may also provide useful information. The concentration, % DMSO, and absorbance wavelength for each dye in NYT-1 are summarized in Table S1.

Array preparation and measurement: Dye test solutions (30 μL) were placed into 384-well assay plates and then metal nitrate solutions (30 μL) were added. After shaking for 10 s in the plate reader, the plate was left for a further five minutes for full color development. The plate picture was taken with the CCD camera and the UV/Vis spectrum was measured by using the plate reader from 350–750 nm at 10 nm intervals.

Data acquisition and basic analysis method: The optimized dye solutions of NYT-1 were placed in 384-well plates (30 μL each) in the order shown in Figures S3A,B. In this format, each dye occupies 2×4 blocks. Next, cation solutions prepared at three different concentrations (30 μL each) were added to the upper three rows, and water was added to the last row as control. The identical two columns provided duplicate experimental data. After 5 min of mixing, the visual image of the plate was recorded with the CCD camera and absorbance spectra were recorded by using the plate reader (350–750 nm at 10 nm intervals). To confirm the reproducibility of the generated data, the same experiment was repeated by using another independent plate on a different day. Thus, a total of four sets of data points were collected and analyzed.

First of all, the visual images before (Figure S3A) and after (Figure S3C) addition of analyte were subtracted by using Photoshop software for quick qualitative visual inspection (Figure S3D). For quantitative analysis, the absorbance values for 41 wavelengths (350–750 nm, every 10 nm) were extracted from the spectral data. The data for analyte treatment were compared to those of control in the forth row from the same column to avoid plate-to-plate deviation. Although simple fold-changes of absorbance from any wavelength(s) could be used for further analysis, data from an arbitrarily chosen single wavelength has poor sensitivity/high noise, and multiple wavelength measurements generate larger data points, which make the analysis process more difficult and complicated. We extracted the absorbance values from λ_{max} to achieve maximum sensitivity, and minimize the data size and noise level. The dye probes were divided into two classes, depending on their responses to analytes. Some dyes changed their absorbance intensity without significant λ_{max} change.

Other dyes showed changes in both absorbance intensity and maximum wavelength. For the first class of dyes (class I), we used the absorbance values at λ_{max} (λ_0) for fold-change calculation (Figure S4 A). If the intensity of the analyte test is I'_0 and that of the control is I_0, the fold-change F can be expressed as follows [Eq. (1)]:

$$F = \frac{I'_0}{I_0} \quad (1)$$

For the second class of dyes (class II), there are two λ_{max}: one for control (λ_1) and a new peak that appeared in the test solution (λ_2) (Figure S4 B). The effective fold-change can be calculated as follows [Eq. (2)]:

$$F = \left(\frac{I_1}{I_2}\right)\left(\frac{I'_2}{I'_1}\right) \quad (2)$$

I_1 and I'_1 refer to the absorbance values at λ_1, and I_2 and I'_2 refer to the absorbance values at λ_2, for which I' values are for the test solution and I values are for the control. In Equation (2), the term $\frac{I_1}{I_2}$ is a normalization factor, with which a nonresponding dye will give $F=1$ (no change).

Although this approach is much more sensitive than the use of values from randomly chosen wavelength(s), if each λ_{max} should be decided for each test separately (maybe manually), the data manipulation is too laborious, especially for massive data treatment. To minimize the work load to a manageable level, we assumed that the wavelengths for each dye (λ_0 for class I dyes and λ_1, λ_2 for class II dyes) can be preset, although the change in wavelength of each dye may depend on the analytes and their concentrations generating various new maximum wavelengths. To test the reliability of this hypothesis, the maximum wavelength change from three concentrations (10, 3.3, 1 mM) of 41 cations (total of 23124 spectra) were analyzed and we found that in 97% of cases (22386), the experimental λ_{max} values match the preset λ_0 or λ_1 or λ_2 values within an error range of 20 nm. Actually, this is a much greater percentage than we expected and means that most of the dyes respond to different analytes in a similar manner in terms of wavelength change, although the quantitative changes in intensity vary. Thus, we can use the change in absorbance near λ_{max} for the majority of the data, and this method will contribute significantly to the high sensitivity of the fold-change while minimizing the data size. The λ_0, λ_1, and λ_2 preset values are summarized in Table S1.

Based on the preset wavelengths, the corresponding absorbance data were extracted by using the macro function of the Excel program, and the fold-changes were calculated according to Equations (1) and (2). The log value of fold-change, "log$F$" was used for further analysis. For visual presentation, the log$F$ data were converted to a heat map (Figure S3 E,G: green indicates the increase and red indicates the decrease of fold-change) and bar graph (Figure S3 F). These two methods present the same data in different formats, from which a clear trend of concentration-dependent pattern changes can be visualized.

Acknowledgement

This work was supported by the National Science Foundation (CHE-0449139). Components of this work were conducted in a Shared Instrumentation Facility constructed with support from Research Facilities Improvement Grant C06 RR-16572 from the NCRR/NIH. J.S.L. was supported by a Korea Research Foundation Grant funded by the Korean government (MOEHRD, Basic Research Promotion Fund: KRF-2005-C00088).

[1] a) F. Feigl, V. Anger, R. E. Oesper, *Spot Tests in Inorganic Analysis, 6th ed.*, Elsevier, Amsterdam, **1972**; b) F. Feigl, V. Anger, R. E. Oesper, *Spot Tests in Organic Analysis, 7th ed.* Elsevier, Amsterdam, **1966**.
[2] D. Drayna, *Annu. Rev. Genomics Hum. Genet.* **2005**, *6*, 217–235.
[3] K. J. Albert, N. S. Lewis, C. L. Schauer, G. A. Sotzing, S. E. Stitzel, T. P. Vaid, D. R. Walt, *Chem. Rev.* **2000**, *100*, 2595–2626.
[4] J. J. Lavigne, E. V. Anslyn, *Angew. Chem.* **2001**, *113*, 3212–3225; *Angew. Chem. Int. Ed.* **2001**, *40*, 3118–3130.
[5] H. Miyaji, J. L. Sessler, *Angew. Chem.* **2001**, *113*, 158–161; *Angew. Chem. Int. Ed.* **2001**, *40*, 154–157.
[6] a) N. A. Rakow, A. Sen, M. C. Janzen, J. P. Ponder, K. S. Suslick, *Angew. Chem.* **2005**, *117*, 4604–4608; *Angew. Chem. Int. Ed.* **2005**, *44*, 4528–4532; b) K. S. Suslick, N. A. Rakow, S. Avijit, *Tetrahedron* **2004**, *60*, 11133–11138.
[7] C. Zhang, K. S. Suslick, *J. Am. Chem. Soc.* **2005**, *127*, 11548–11549.
[8] T. Mary, C. Igel, G. Liebsch, I. Klimant, O. S. Wolfbeis, *Anal. Chem.* **2003**, *75*, 4389–4396.
[9] E. Mueller-Ackermann, U. Panne, R. Niessner, *Anal. Methods Instrum.* **1995**, *3*, 182–189.
[10] H. Prestel, A. Gahr, R. Niessner, *Fresenius J. Anal. Chem.* **2000**, *368*, 182–191.
[11] D. Mikami, T. Ohki, K. Yamaji, S. Ishihara, D. Citterio, M. Hagiwara, K. Suzuki, *Anal. Chem.* **2004**, *76*, 5726–5733.
[12] a) I. T. Jolliffe, *Principal Component Analysis*, Springer, New York, **1986**; b) K. Y. Yeung, W. L. Ruzzo, *Bioinformatics* **2001**, *17*, 763–774.
[13] E. Blalock, *A Beginner's Guide to Microarray*, Kluwer, New York, **2003**.
[14] T. M. Cover, P. E. Hart, *IEEE Trans. Inf. Theory* **1967**, *13*, 21–27.

Received: March 6, 2006
Published online: May 22, 2006

